Polymer Testing 135 (2024) 108472

Contents lists available at ScienceDirect

Polymer Testing

journal homepage: www.elsevier.com/locate/polytest

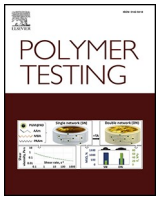

Effect of repeated salt fog-dry cycles on the performances reversibility of flax fiber reinforced composites

V. Fiore [a,*], L. Calabrese [b], C. Sanfilippo [a], E. Proverbio [b], A. Valenza [a]

[a] Department of Engineering, University of Palermo, Viale Delle Scienze, Edificio 6, 90128, Palermo, Italy
[b] Department of Engineering, University of Messina, Contrada Di Dio (Sant'Agata), 98166, Messina, Italy

ARTICLE INFO

Keywords:
A. polymer-matrix composites (PMCs)
B. Environmental degradation
D. Mechanical testing
Repeated aging cycles
Moisture desorption
Flax fibers

ABSTRACT

This paper aims to evaluate the effectiveness of flax fiber reinforced epoxy composites (FFRCs) under realistic environmental conditions, contributing to the development of sustainable composite materials for semi-structural outdoor applications. For this purpose, the reversibility of FFRC performance under consecutive and repeated humid-dry aging cycles was investigated for the first time.

In particular, FFRCs were exposed to three cycles (total aging time of 12 weeks), with each cycle (duration 4 weeks) comprising 10 days of wetting (salt-fog spray; 35 °C, 95 % RH, 5 wt% NaCl solution) and 18 days of drying (22 °C, 50 % RH). Three-point bending tests were carried out up to 18 days of drying within each cycle to monitor changes in the mechanical performances of composites. Water absorption capacity, density and void content were also assessed by tracking weight changes throughout the aging campaign. The experimental results highlighted that the humid phase of each cycle causes degradation of FFRC materials, even though they are able to fully recover their flexural strength during each dry phase, indicating reversible aging. On the other hand, a stiffness permanent reduction was observed due to irreversible degradation phenomena.

1. Introduction

In recent years, natural fiber reinforced composites (NFRCs) have garnered increasing attention due to their promising potential to bridge the gap between satisfying mechanical properties and environmental sustainability. This convergence of strengths makes NFRCs an exciting field of research and development [1].

The increased interest in NFRCs originates from their ability to fulfill the need for strong, durable, and eco-friendly materials [2]. Unlike traditional synthetic fiber composites, NFRCs use renewable plant fibers like flax, hemp, jute, and kenaf, aligning with the global trend toward sustainable production [3]. Different types of fabrics can be used as reinforcement of NFRCs [4–6] These composites are often characterized by tensile strength, flexural strength, and impact resistance, resistance making them suitable for structural semi-structural applications [7]. Additionally, NFRCs often exhibit superior damping properties in comparison to their synthetic counterparts, making them suitable for applications where vibration and noise reduction are crucial [3,8].

However, some drawbacks related to the heterogeneity of natural fibers, their weak interfacial adhesion with polymeric matrices and their considerable moisture absorption, restrict the extensive use of these materials. This limitation is particularly evident in outdoor applications where alternate wet or humid conditions are prevalent. These factors hinder the widespread diffusion of natural fibers, making them less suitable for use in such conditions.

While an extensive literature is available on evaluating and predicting the behavior of natural fiber reinforced composites exposed to humid or alternate humid/dry conditions [9–13], few studies explored the recovery of these materials after drying.

Kim and Seo [14] investigated the evolution of mechanical properties as well as the water absorption of sisal fiber reinforced composites under alternate aging tests. In particular, these composites were first immersed in water for 9 days, then dried at 50 °C for 1 day, showing that increased cyclic times led to higher water uptake and poorer mechanical properties (i.e., decreased maximum strength and severe elongation).

The impact of cycles of UV radiation at 70 °C (8 h) and water condensation at 50 °C (4 h) on the aging resistance of three types (unidirectional, cross-ply and quasi-isotropic) of biocomposites made of green epoxy matrix reinforced by sisal fibers was studied by Zuccarello et al. [15]. It was found that both the tensile strength and the delamination strength of these biocomposites were significantly influenced by the aging after undergoing 112 cycles over a total of 8 weeks.

* Corresponding author.
E-mail address: vincenzo.fiore@unipa.it (V. Fiore).

https://doi.org/10.1016/j.polymertesting.2024.108472
Received 5 April 2024; Received in revised form 16 May 2024; Accepted 30 May 2024
Available online 31 May 2024

Cadu et al. [16] investigated the effect of wet-dry cycles (i.e., 90 % HR for 3.5 days and 40 % HR for a further 3.5 days, both at 55 °C) on unidirectional flax/epoxy composites. After 1 year and 52 aging cycles, the composite showed slight declines in mechanical performances (i.e., −10 % in moduli and −14 % in the ultimate tensile stress). Furthermore, other authors assessed the impact of aging on composite transverse properties [17]. Results revealed significant decreases in both tensile strength (i.e., about −20 % after 1 week) and modulus (i.e., approximately −18 % after 1 week, reaching −45 % after 1 year). These findings were mainly attributed to physical matrix plasticization.

Analogously, Mak et al. [18] investigated the tensile performances reduction of flax fiber reinforced polymers subjected to 12 wet-dry cycles, showing that aging cycles caused a significant reduction in mechanical properties already after 3 aging cycles.

Furthermore, Barbière et al. compared the effect of ambient, wet and wet/dry conditions (i.e., water immersion at room temperature more than 90 days followed by drying at 40 °C for 2 days) on the fatigue behavior of hemp/epoxy composites showing that the evolution of cumulative AE energy and hysteresis loop energy, the evolution of damage quantity and final hysteresis energy are very similar regardless of the conditioning [19].

In such a context, in the last years our attention was focused on the assessment of the effects of reversible and irreversible degradation phenomena on performances of glass, flax and glass-flax fiber reinforced epoxy composites during their exposition to discontinuous marine conditions [20–26].

In particular, a detailed investigation addressed to evaluate the ability to recover the physical and mechanical properties of epoxy based composites reinforced with flax fibers, exposed to a single humid-dry cycle (i.e., salt-fog exposure for 15 and 30 days, followed by 21 days of controlled dry storage) was carried out [21,26]. The main findings evidenced that these composites experience both reversible and irreversible aging phenomena during the initial humid phase in addition to a noticeable regaining of their mechanical properties during the following dry phase, especially for short humid cycles. Generally, it was shown that that their mechanical strength is mainly affected by reversible degradation phenomena while stiffness is influenced by irreversible degradation: i.e., both impacting the composites toughness evolution during the wet/dry cycle.

Overall, these results made us infer that further research activities focused on assessing performances of FFRCs aged in hydrothermal or wet/dry environmental conditions will allow to improve our knowledge of their real durability when exposed to hostile environments. In particular, the reversibility of the performance's recovery of these composites under consecutive and repeated cycles of exposure to salt spray and dry phases is not a well-studied topic. Investigating this could provide significant added value and contribute to a deeper understanding in this research field.

For these reasons, the present work aims to evaluate, for the first time, how three repeated humid-dry aging cycles can impact the reversibility of physical and mechanical properties of flax fiber-reinforced epoxy composites (FFRCs), manufactured through vacuum assisted resin infusion process. Specifically, the maximum aging period was 12 weeks, with each humid-dry cycle lasting four weeks (i.e., 10 days of wetting followed by 18 days of drying). For each cycle, three-point bending tests were performed after 0, 5, 10, and 18 days of drying. Furthermore, the composites' weight was monitored at regular intervals during both humid and dry phases of each cycle, to assess the variation in their physical properties, such as water absorption capacity and density.

2. Experimental

2.1. Materials and methods

Flax fiber reinforced polymer (FFRP) panels (30 × 30 × 0.335 cm^3) were produced via vacuum assisted resin infusion technique. A two-stage vacuum pump model VE 235 D by Eurovacuum (Reeuwijk, Netherlands) was employed to apply a vacuum level equal to 0.1 atm (absolute). Each composite underwent a first curing phase at room temperature (25 °C ± 1 °C) for 24 h followed by post-curing at 50 °C for 15 h. A commercial DEGBA epoxy resin (SX8 EVO supplied by Mates Italiana s. r.l., Italy) mixed with its amine-based hardener (100:30 by weight) was used as polymeric matrix. Five 2 × 2 twill weave woven flax fabrics (shown in Fig. 1) with nominal areal weight of 318 g/m^2 (Lineo, France), constituted the reinforcement of composites. These fabrics were employed in the composite manufacturing process in their as-received state (i.e., without undergoing any pre-treatment).

The fiber volume fraction of the manufactured composite was equal to 36.8 %. This value was calculated through the following equation [27]:

$$v_f = 100 \times \left(\frac{n \times m}{\rho_f \times t}\right)$$

where n is the number of fabric layers, m is the fabric nominal areal weight, ρ_f is the density of flax fibers (i.e., 1.29 g/cm^3) and t is the composite's thickness.

2.2. Salt-fog/dry aging phases

This work aims to determine the influence of three consecutive humid/dry aging cycle on the ability of FFRCs to regain their mechanical performance after exposure to these conditions, mimicking those encountered in the marine field.

During the humid phase, a climatic chamber model CC1000iP (Ascott analytical, UK) was used to subject composite panels to salt-fog spray (5 wt% NaCl solution) up to 10 days at 35 °C ± 1 °C, according to ASTM B 117 standard. After this exposure period, five samples for each condition were cut to their nominal size (as required for the specific test) with the aid of a diamond saw. The aged specimens were then stored in a dry environment (50 % relative humidity and 22 °C temperature) up to 18 days before undergoing mechanical testing. Hence, each cycle lasted 28 days (i.e., it consists of a 10 days humid phase and an 18 days drying phase) and the entire aging campaign was characterized by 3 humid/dry cycles. In more detail, three-point bending tests were conducted after 0, 5, 10, and 18 days of drying for each cycle in order to monitor changes in the mechanical performances of biocomposites.

For the sake of clarity, specimens will be named using the code "nWDb", where n and b represent the cycle number (i.e., 1, 2 or 3) and the time intervals in days of the dry phase, respectively. For example,

Fig. 1. Twill weave flax fabric.

2WD7 is referred to specimens tested after 7 days of drying during the second cycle. As reference, 0WD0 indicates unaged specimens (control sample).

2.3. Water uptake measurements

To determine the relationship between water absorption and salt-fog exposure time, following the ASTM D570 standard, three square samples (100 mm × 100 mm) were daily removed from the salt-fog chamber up to 10 days, wiped with a dry cloth and weighed using an analytical balance (model AX 224 by Sartorius, Germany) with a precision of 0.1 mg. The weight change (WC, expressed in percentage) of composites was calculated using the following equation:

$$WC(\%) = \frac{W_{ti} - W_0}{W_0} \bullet 100 \quad \text{Eq. 1}$$

Where W_0 represents the weight of unaged samples and W_{ti} is the weight of the sample after at *ti* aging exposure time (i.e., identified as sum of the time intervals in salt-fog chamber and drying). The same formula was used to monitor also the weight reduction occurring during the dry phases of each cycle, by weighing samples every day.

In addition, the density of composites after aging was measured during the water uptake test. The experimental density (ρ_{ce}) of each sample was calculated by taking the mean value of three weight and volume measurements. All the standard deviations in these measurements were below 0.015 g/cm^3, thus indicating good consistency.

2.4. Quasi-static mechanical tests

For each investigated condition, five specimens (13 mm × 64 mm) were subjected to three-point bending tests in accordance to ASTM D 790 standard, by using a U.T.M. model Z005 by Zwick-Roell, Germany, equipped with a 5 kN load cell. The support distance and the crosshead speed were fixed at 54 mm and 1.4 mm/min, respectively.

The morphology of the fractured surfaces of samples was observed with the aid of a scanning electron microscopy (SEM, Quanta 450, USA). All analyzed surfaces were preliminary sputtered with a thin layer of gold to prevent electrostatic charging during the measurements.

Fig. 2 schematizes the manufacturing process of composites, the aging cycles applied and the main characterization analyses (i.e., water uptake and flexural tests).

3. Results and discussion

3.1. Water uptake measurements

Fig. 3 depicts the weight change experienced by flax composites, due to water absorption and desorption experienced in salt-fog and dry phases of each aging cycle.

By evaluating the first cycle on this graph, it is possible to notice that when the composite material is exposed to salt-fog spray conditions (i.e., humid phase), its weight gradually increases over time with a steeper rate of increase in the early stages of exposure. This initial rapid water uptake can lead to a weight gain of over 4 % after just 2 days (48 h) of salt-fog exposition. However, as the exposure time continues, the rate of water absorption slows down, thus resulting in a less pronounced weight gain trend. A bimodal trend with a knee in correspondence of around 150 h can be identified.

In particular, the flax fiber reinforced composite achieves a maximum weight change equal to 7.89 % after 10 days of exposition (i.e., 240 h). This behavior ca be attributed to a combination of factors that enhance the absorption of water experienced by FFRC materials. The hydrophilicity of the composite components promotes water absorption on the surface, initiating the uptake process. In more detail, water molecules are able to interact with unreacted hydrophilic and polar groups of the thermoset matrix, including hydroxyl and amine groups, creating favorable pathways for water diffusion [28,29]. Flax fibers' hydrophilic behavior notably accelerates the amount of water absorbed

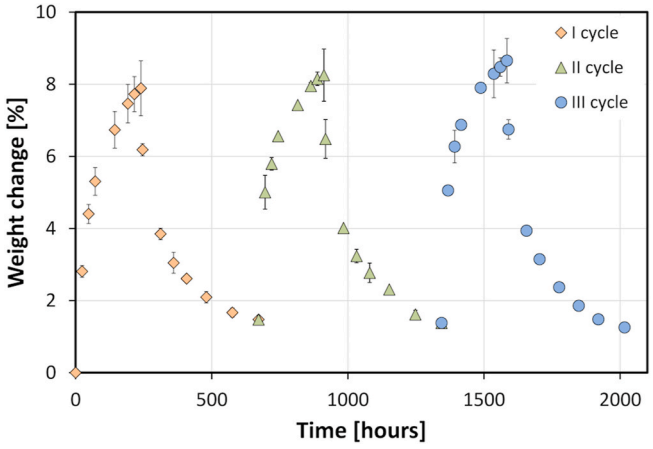

Fig. 3. Weight change evolution at increasing time during each aging cycles.

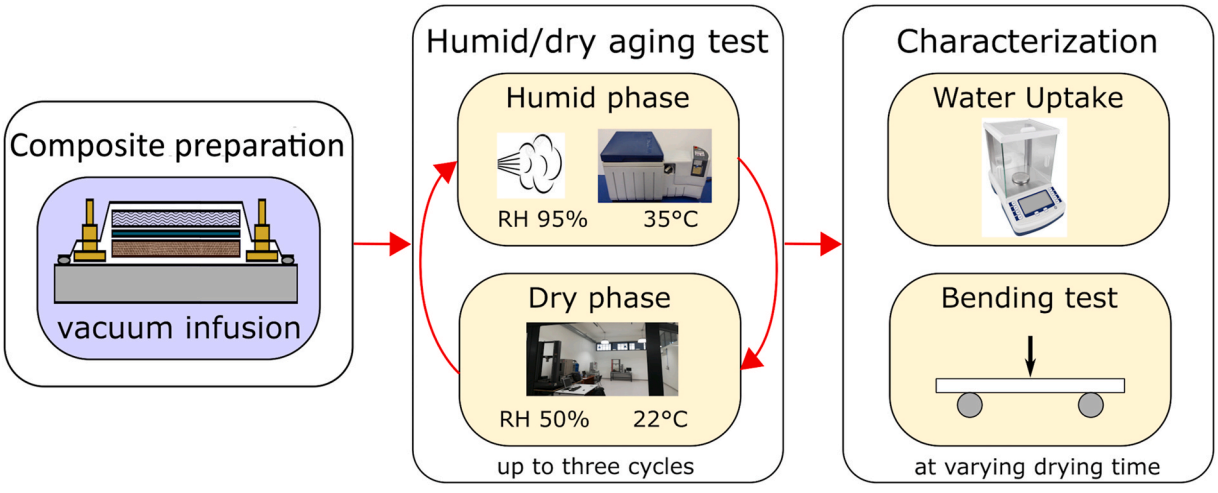

Fig. 2. Flowchart of the experimental campaign.

by composites exposed to humid or wet conditions [20,30]. This process involves three main stages [31,32]: (1) water diffusion through micro-cavities and pores on the matrix surface, (2) enhanced water diffusion driven by capillary action at the fiber-matrix interface, and (3) fiber-matrix debonding and matrix cracking caused by aging-induced phenomena like fiber swelling and matrix softening [33]. Additionally, water absorption disrupts secondary cellulose bonds within flax fibers, thus weakening them and creating pathways for further water penetration [21,34].

The weight gain of the composite can be attributed to a dynamic competition among several concurrent processes. In the second part of the water adsorption step, characterized by a lower slope in the water uptake trend, slow kinetic processes become the main limiting factors. This agrees with the bimodal curve trend, that deviates from the typical Fickian behavior, cause of irreversible damage and water absorption over time [35].

Further interesting considerations can be argued evaluating the evolution of the weight change during the next humid-dry cycles. Both the second and the third cycle show an analogous monotone trend with a progressive increase during the humid phase followed a reduction in weight during the next dry phase. Nevertheless, some differences may be found in the amount of weight gained or lost during these phases. In particular, it is possible to observe an increase in the maximum water uptake values shown at the end of humid phase at increasing the cycle number. These values in the second and third cycles are equal to 8.25 % (i.e., after 912 h of aging) and 8.65 % (i.e., after 1584 h of aging), respectively. Analogously, the residual weight change at the end of dry phases of II cycle and III cycle are equal to 1.38 % (i.e., after 1344 h of aging) and 1.25 % (i.e., after 2016 h of aging), respectively. Therefore, an increase in the gap (Δw) between maximum and minimum weight values reached at the end of humid and dry phases is found as function of the aging cycle' number, as reported in Table 1. This implies that the FFRCs show great predisposition to absorb and desorb water leading to a wide Δw at increasing the cycles' number.

This behavior can be due to the degradation phenomena occurring during the humid phase of each cycle. Due to water adsorption and diffusion into the bulk material, the microstructure of FFRC changes due the activation and growth of microcracks and/or interfacial debonding. This modification becomes more significant with an increasing number of applied aging cycle.

Accordingly, Newman in Ref. [36] evidenced that the water damaging can be ascribed to an increased volume of pores, that led to a relevant increase in water diffusivity of aged samples.

Due to the prolonged exposure to salt-fog, the specimens experienced somewhat significant physical damages [36]. These defects, such as internal cracks, behave as preferential pathways through which water can diffuse, thus worsening the deterioration of the composite' structure [37] speeding up the permeation (i.e., during the humid phase) and the evaporation (i.e., during the following dry phase) of the absorbed water. Hence, the triggering of these microcracks or debonding areas at the fiber-matrix interfaces within the composite [38] is responsible for the acceleration of these reversible processes, as well as the effective sorption and subsequent removal of absorbed water through evaporation [21].

Furthermore, to assess better the degradation of composites exposed to salt-fog, the evaluation of their density under varying humid/dry exposure times can provide valuable insights into these degradation processes.

In this regard, Fig. 4 displays the variation of composite's density during the entire aging campaign.

The growing trend during the humid phase suggests that water is gradually being absorbed by the material. For example, the 1WD0 samples (i.e., exposed to salt-fog spray conditions for 10 days without subsequent drying) show density increase (i.e., +4.6 %) in comparison to the unaged samples (i.e., 1.184 g/cm^3 and 1.132 g/cm^3, respectively). This means that water is accumulating in both the hydrophilic and porous regions of the composite. After two and three salt-fog phases (2WD0 and 3WD0, respectively), the density increases are reduced to 1.174 g/cm^3 and 1.172 g/cm^3, respectively.

Furthermore, the drying behavior of the composite depends on the duration of their salt-fog exposure. 1WDx, 2WDx and 2WDx represent specimens exposed for one, two or three cycles in the salt-fog chamber followed by drying at different times, respectively. 1WDx batch initially absorbs water during the humid phase, thus leading to an improvement of composite density. Afterward, the density suddenly decreases during the dry phase until reaching a stable level of 1.128 g/cm^3 after prolonged drying.

3WDx batch starts with about 1 % lower density than 1WDx. However, it loses water significantly within already the first 24 h of drying, reducing its density by 1.7 % (i.e., from 1.172 g/cm^3 to 1.153 g/cm^3). After further drying, it reaches a plateau at around 1.115 g/cm^3. This suggests that most absorbed water is easily released, but some permanent damage might occur, as indicated by the remaining weight gain even after prolonged drying time. In fact, upon analysis, it was discovered that the value derived from the aged specimen was slightly lower than that the unaged counterpart. This discrepancy may suggest that the humid/dry aging treatment triggered the nucleation of various voids or cavities inside the bulk composite structure (i.e., mainly at the fiber-matrix-interface). Due to these newly formed defects, the apparent density of aged specimens underwent a decrease towards the end of the dry phase of each cycle when compared to the unaged specimen. This implies that the aging treatment exerted a notable influence on the material, thus resulting in altered physical properties.

Table 1
Main weight changes at varying aging cycles.

	Maximum weight change [%]	Residual weight change [%]	Δw [%]
I Cycle	7.89	1.47	6.41
II Cycle	8.25	1.38	6.87
III Cycle	8.65	1.25	7.40

3.2. *Quasi-static mechanical tests*

3.2.1. *Stress-strain curves*

In order to provide a reliable benchmark for assessing the mechanical performance modification in flax composites during humid and dry phases, an analysis was performed to evaluate the changes in flexural stress-strain curves over different periods of exposure to salt-fog and dry conditions, which represents the humid and dry phases. This analysis is depicted in Fig. 5, and it serves as a preliminary contribution of the relationship between aging conditions and mechanical behavior of the flax composite.

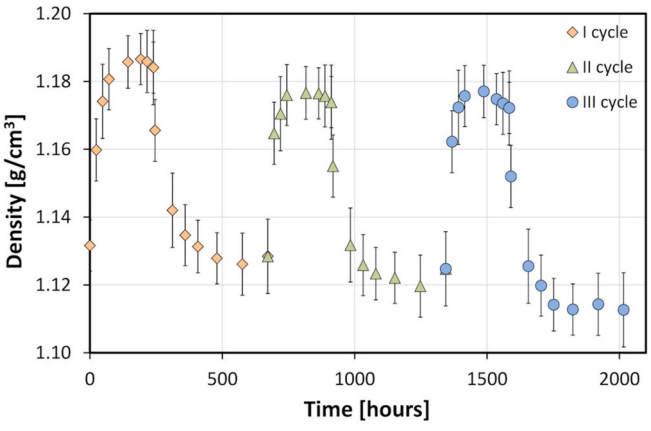

Fig. 4. Density evolution at increasing time during each aging cycles.

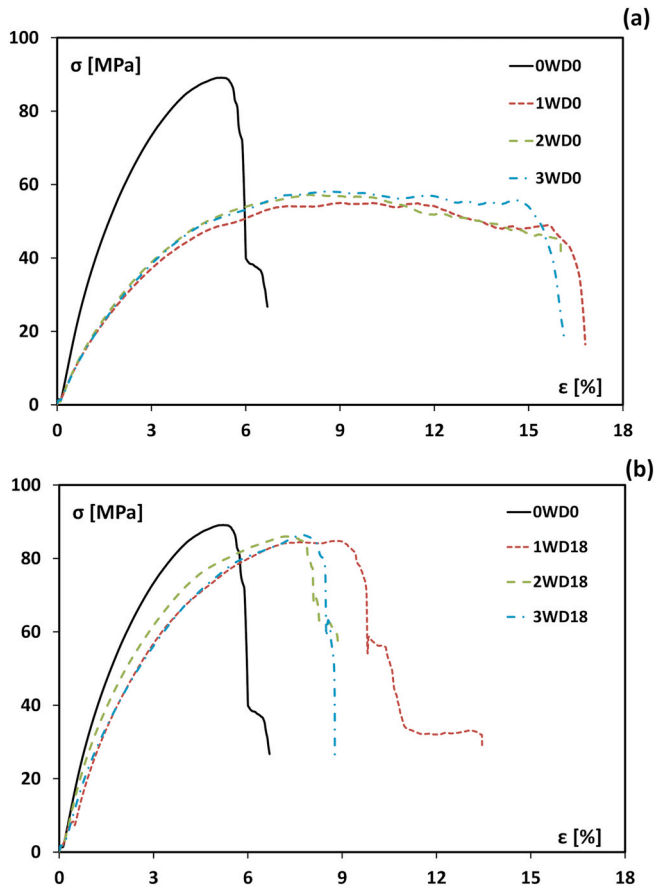

Fig. 5. Stress-strain curves at the end of (a) humid phase and (b) dry phase for each cycle. Unaged sample was added as reference.

By evaluating the stress-strain curves referred to samples immediately after the exposition to salt-fog chamber (Fig. 5a) an evident reduction in strength and stiffness in the aged samples can be identified, compared to the unaged one. This can be observed by an evident reduction of the maximum stress and the slope of the curves at low strain, related to strength and stiffness of the composite, respectively. Furthermore, due to exposition to the humid environment the composite acquires a clear elastoplastic behavior, as identifiable by a large deflection of the stress-strain curve at large strain. Due to exposure to salt-fog, a transition from mainly linear mode, characterized by a sudden and catastrophic failure, to non-linear one that entails progressive failure, occurs. This could imply the presence of extensive interlaminar damages within the investigated composites, leading to the formation of shear/delamination fractures, ultimately resulting in a ductile failure mode [39]. Therefore, the observed changes in fracture behavior reflect the negative effects of salt-fog exposition on the composites, highlighting the critical role of interlaminar damages in governing their structural integrity.

However, by comparing the curves at different aging cycles, it is found that the mechanical properties are not particularly influenced by this factor. All specimens show very similar main mechanical properties, with a reduction in strength of 35 %. At the same time, all aged specimens exhibit the failure strain about 3 times higher than that found for the unaged specimen (~16 % and 5.8 %, respectively).

It is important to underline that not all aging processes cause permanent damage to composite laminates. As Fig. 3 clearly illustrates, the dry phase conducted in controlled conditions (i.e., 50 % RH at 22 °C) concerns the gradual removal of water absorbed during the humid phase. After this, a gradual recovery of mechanical properties is predictable, taking into account that some of the degradation processes might be reversible. Identifying and quantifying the extent of this reversibility experienced throughout the dry phase is crucial for designing composites with enhanced durability.

Fig. 5b compares the stress-strain curves shown by composites at the end of each dry phase of the three cycles. As previously mentioned, exposure to salt-fog conditions significantly decreased flexural strength, stiffness, and strain at break for 1WD0, 2WD0, and 3WD0 composites. However, a subsequent drying phase led to a partial recovery of these performances. Post-drying flexural stress-strain curves exhibited enhanced maximum strength and reduced strain at failure. Additionally, the initial slope of the curve (corresponding to flexural modulus), evaluated at low strain values, also increased.

This indicates that the detrimental effects of water exposition, such as plasticization and softening, can be partially reversed upon drying. Specifically, the composite's maximum flexural strength nearly recovered after drying. For instance, the 1WD18 sample exhibited an average maximum flexural strength of 84.8 MPa, which is only 5 % lower than that of the unaged sample (i.e., 0WD0). Instead, the 1WD18 sample's strain at failure reached 9.7 %, significantly greater that the 0WD0 sample's value by 3.9 %. Similar observations were made for the 2WD18 and 3WD18 samples.

During the humid phase, when water is absorbed, a range of degradation mechanisms affecting the mechanical behavior of composites in different manners trigger. It is interesting to note that even after drying, the flax fiber reinforced composite retains its large deflection, suggesting that its stiffness and deformation at break have only been partially compromised. On the other hand, the maximum strength seems to have almost fully recovered. These observations indicate that the decrease in strength during the humid phase is primarily due to reversible aging, while the loss of stiffness is likely a result of a combination of reversible and irreversible processes. Overall, the water absorption during the humid phase has complex effects on the mechanical properties of the composites, with some compromises in stiffness and strength that are partially recoverable. These findings emphasize the importance of understanding the occurring different degradation mechanisms in order to optimize the performance and durability of such composites.

To acquire further information concerning the composites' mechanical changes due to humid/dry aging cycles, Fig. 6 shows morphological SEM images of fractured specimens from the flexural test.

The unaged sample (i.e., 0WD0) may indicate a good compatibility between flax fibers and surrounding polymer. The resin fills the gaps between the fibers, creating a suitable interfacial adhesion and even stress distribution at the fiber/matrix interface. This helps prevent cavities and weaknesses in the material. Upon closer inspection, it becomes evident that the aged sample, (i.e., 3WD18), exhibits characteristics that contrast with its initial state. Specifically, a noticeable change is observed in -flax fibers, which appear prone to unraveling, indicating a potential deterioration in the structural integrity. Furthermore, the apparent loss of interfacial bonding within the fiber-matrix composite can be identified, hinting at a probable cause related to absorbed water. This excess moisture likely contributes to a weakening of the interfacial adhesion, ultimately leading to debonding phenomena occurring at the interface domain [40]. Therefore, the formation of preferential water pathways at the interface between the debonded area further contributes to weaken the adhesion. These structural discontinuities, formed during the humid phase, persist even as the environment transitions into the dry phase, become more relevant with increasing cycle number. As a result, interfacial stress transfer is limited, reducing the stiffness of the composite and improving its ductility and toughness [41,42].

3.2.2. *Flexural strength and stiffness evolution*

A support for a greater understanding of the reversibility/irreversibility of the degradation processes during humid-dry cycles can be provided by analyzing the evolution of flexural strength and modulus values with the aging time (Fig. 7).

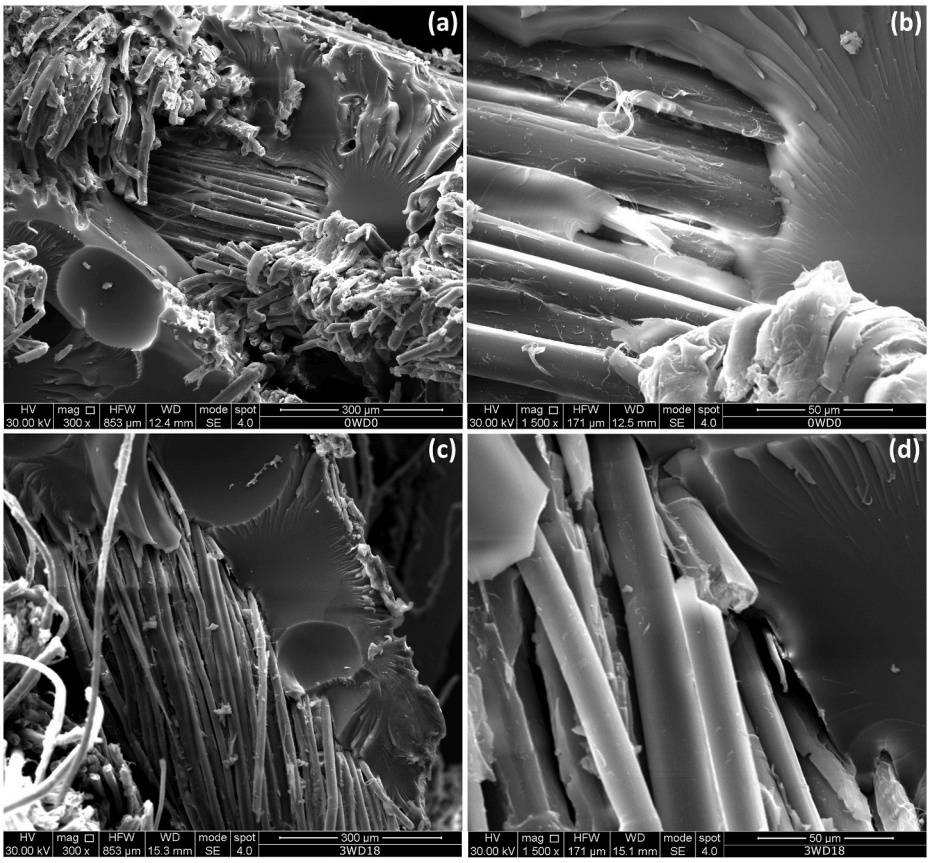

Fig. 6. SEM micrographs at different magnification of fractured surfaces of (a–b) 0WD0 and (c–d) 3WD18 samples.

The composite cyclically undergoes a progressive reduction in strength and stiffness during the humid phase, regaining them during the subsequent dry phase. The results obtained at various drying intervals highlight how the mechanical performances can be largely restored even after a few days of exposure to a dry environment. Regardless of the aging cycle, approximately 20–30 % of the composite's strength is recovered already after 5 drying days (Fig. 7a). This indicates that the degradation phenomena responsible for the decay of the composite's strength during the humid phase are mainly reversible. However, Fig. 7b shows that although the modulus of the composite also increases clearly in value as the drying time increases, it always remains significantly lower than that of unaged specimen. At the end of aging campaign, the flexural modulus shown by flax composite is equal to 3.16 GPa, about −24 % than the unaged material (i.e., 4.18 GPa).

This behavior can be ascribed to diverse degradative phenomena le which play a crucial role in the worsening of the composites' overall performances. In particular, the absorbed moisture alters flax fiber composites' mechanical response. The water absorption could induce swelling of the hydrophilic flax fibers, triggering matrix microcracking [22]. This favors local stresses in the composite mainly located on fiber-matrix interface, which further promote crack initiation and propagation [30].

In this case the reduced exposure in salt spray (i.e., 10 days) may not allow the formation of significant amount of microcracks. This would lead to non-degenerative degradation phenomena which can be reversibly recovered whether the specimens are removed from the humid environment.

Likewise, the decrease in the stiffness can generally be related with softening and plasticization phenomena induced in wet NFRCs [43]. In fact, the stiffness drop is likely due to a combined effect of both matrix and fiber softening. This happens because dry flax fibers have very stiff cellulose fibrils, where the cellulose molecules are tightly bound together. However, water can seep through these fibers and interact with the hydroxyl groups on the cellulose molecules, creating weak hydrogen bonds [44]. This weakens the bonds that hold the flax structure rigid, acting like a lubricant also allowing the cellulose molecules to freely move, making the fibers more flexible [45].

Furthermore, from the matrix point of view, epoxy resins can absorb both free and bound water [46]. Free water molecules have large mobility, diffusing freely through the gaps and holes within the bulk of the thermoset structure, thus leading to a reversible sorption effect. In contrast, bound water molecules are constrained by interaction to the polar groups within the polymer network, thus leading to permanent sorption effects [47].

Fig. 8 shows the overlap of drying curves in different cycle, after aligning the axes with the beginning of the drying phase for each cycle. This helps to visualize how the recovery of mechanical performance changes depending on the aging cycle.

Both mechanical performances have been normalized to the values shown by the unaged composite, according to the following equations:

$$FSV(\%) = \frac{\sigma_{ti} - \sigma_0}{\sigma_0} \bullet 100 \quad \text{Eq. 2}$$

$$YMV(\%) = \frac{E_{ti} - E_0}{E_0} \bullet 100 \quad \text{Eq. 3}$$

Where σ_0 and E_0 represent flexural strength and modulus at the beginning of the aging campaign (i.e., dry unaged samples), respectively. On the other hand, σ_{ti} and E_{ti} are the flexural properties shown by the flax fiber reinforced composite at t_i aging exposure time (i.e., identified as the sum of the time intervals in salt-fog chamber and drying), respectively.

According to Fig. 8a, the FSV index values at 0 time decreases at increasing aging cycles. These points represent the flexural strength of

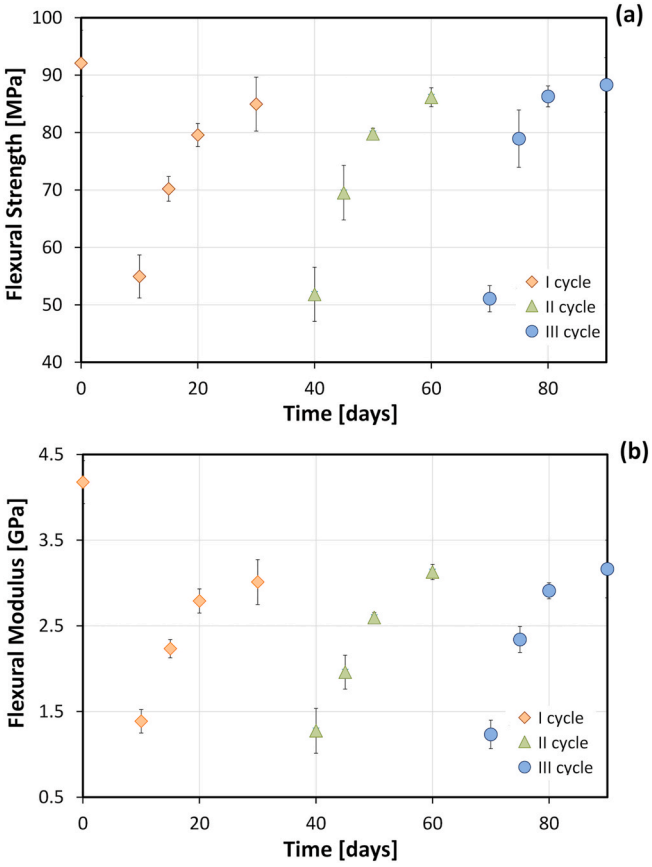

Fig. 7. Evolution of flexural (a) strength and (b) modulus values at increasing time during each aging cycle.

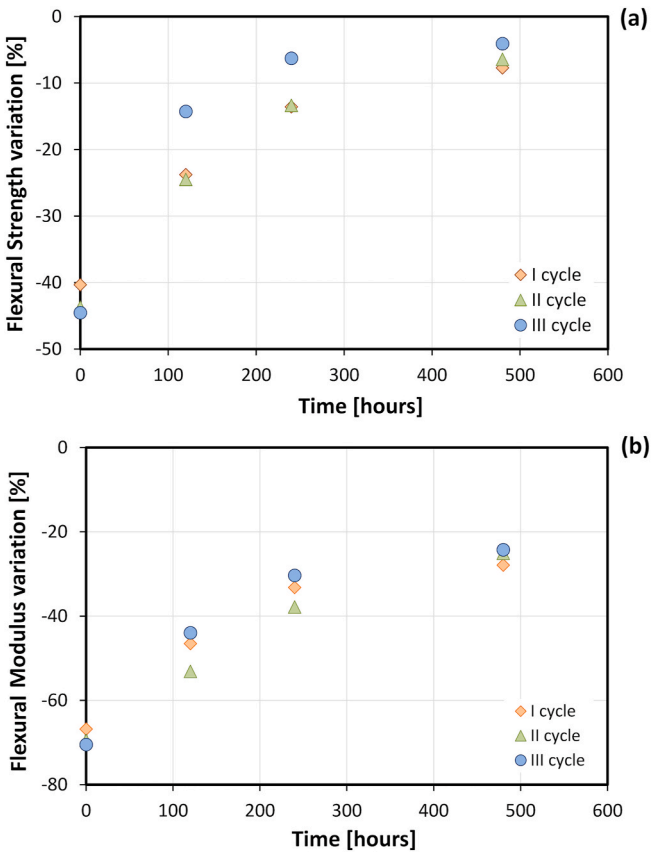

Fig. 8. Percentage variations of flexural (a) strength and (b) modulus at increasing time during each aging cycle.

samples immediately after the exposure to salt-fog in each cycle (i.e., 1WD0, 2WD0, and 3WD0 samples). The y-axis values indicate a significant reduction in flexural strength, reaching a maximum decline of 44.5 % for 3WD0 samples.

With prolonged drying, the difference in flexural strength between aged and unaged samples diminishes, as reflected by the decreasing variation in flexural strength values.

Interestingly, although three-cycle tests are characterized by a more significant reduction in resistance, at the same time they show faster recovery. This means that despite experiencing a considerable decrease in the strength, the composite is able to regain much of its original mechanical strength relatively quickly. Indeed, after about 240 h of drying, the overall mechanical resistance of flax fiber reinforced composite is only −6.28 % lower than that of the unaged specimen, indicating its effective recovery capabilities over time.

Analogous consideration can be argued evaluating Fig. 8b referred to YMV index. It is worth noting that the flax fiber reinforced composite with the most rapid recovery capacity is the one that has undergone three aging cycles. It is interesting to observe that, unlike the strength trend, the NFRC indicates a residual significant modification in the flexural modulus. Specifically, (i.e., 3WD18 sample), the flexural modulus at the end of the final drying cycle is found to be −24.3 % lower than the initial value (i.e., shown by the unaged counterpart). Such findings shed light on the unique properties and characteristics of various FFRP materials, highlighting the influence of aging cycles on the mechanical performances of the composite, specifically on its flexural stiffness.

These considerations are summarized in Table 2 where FSV and YMV indices at varying aging cycles are compared.

At increasing aging cycles, the minimum FSV and YMV increases as a consequence of the larger hydrothermal aging induced by salt-fog environment. All these degradation phenomena are largely reversible as confirmed by the residual FSV and YMV indices that progressively increase toward zero value with increasing aging cycles. In particular, these parameters diminished to 3.64–3.65 % at the end of the third cycle. This implies that the reversible contribution of the degradation phenomena (related to ΔFSV and ΔYMV values) becomes increasingly predominant compared to the irreversible ones (related with residual FSV and YMV values).

To visually depict the degradation extent of the examined composite (considering FSV and YMV indices), Fig. 9a and b present topological maps relating the flexural strength variation index FSV and Young modulus variation index YMV at increasing time, respectively. These graphs aid in comprehending whether the degradation can be fully or partially regained during each dry phase of the aging cycles and how these phenomena evolve due to aging.

For each plot, the colored lines are referred to low or long aging cycles. The vertex of the lines indicates the transition from humid to dry cycle. During the drying time, two distinct subsections, able of distinguishing between irreversible and reversible aging regions, were identified. Furthermore, the differences between lowest and highest aging cycles (I and III cycles, respectively) were highlighted in the map with red arrows. Besides, the topological maps allow to indicate the recovery envelope curves, related with the composites' increasing performance recovery during the humid/dry cycles. Summarizing, some considerations can be argued from the identified sub-areas.

1. Reversible aging area. This states the performance lost during exposure to high humidity conditions, which is reversibly recovered by removing the composite from this environment and restoring ambient dry conditions. This region is strictly correlated to degradative phenomena (e.g. water adsorption within the polymer

Table 2
Flexural strength and modulus variations at varying aging cycles.

	Minimum FSV [%]	Residual FSV [%]	Δ FSV [%]	Minimum YMV [%]	Residual YMV [%]	Δ YMV [%]
I Cycle	−40.3	−7.7	32.6	−66.8	−27.9	38.9
II Cycle	−43.7	−6.4	37.3	−69.5	−25.1	44.4
III Cycle	−44.5	−4.1	40.4	−70.5	−24.1	46.2

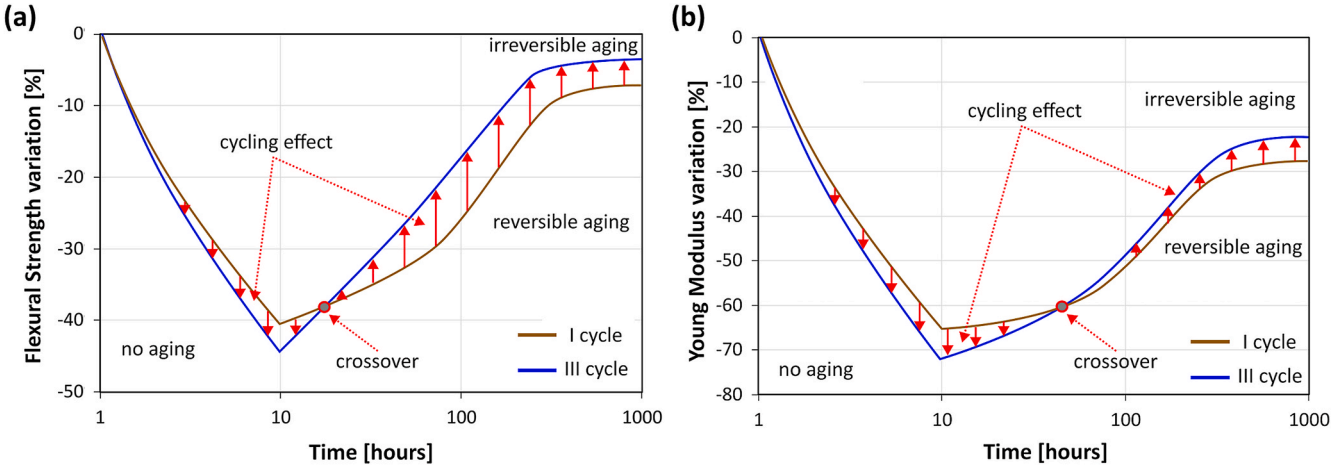

Fig. 9. Topological map of reversible and irreversible aging based on a) FSV and b) YMV indices.

matrix), that weaken the composite, causing it to acquire an elasto-plastic mechanical behavior [23]. The absorbed water can be expelled through natural evaporation during a subsequent drying period, without causing permanent damage to the composite [26];

2. Irreversible aging area. The detrimental effects that endure after removing composites from the climatic chamber (i.e., salt-fog) are due to irreversible phenomena. Delamination, debonding and/or matrix microcracks are damages caused by this degradation [48]. In fact, composites retain these defects at the end of the single cycle (i.e., salt-fog exposition followed by controlled drying), leading to a structural discontinuity and irreversible reduction in their mechanical response [24];
3. Cycling effect area. As the number of aging cycles increases, the performance decay and recovery curve exhibit a graphical twist. Specifically, a reduction during the humid phase and a subsequent larger recovery during the dry phase take place. Consequently, it is possible to identify a crossover point, at which there is a reversal of the trend between the two phases. Furthermore, it is possible to observe that the cycling effect is more relevant to resistance than stiffness plot, allowing to achieve at III aging cycle a very limited irreversible aging area. In fact, this area is very confined in the upper right corner of Fig. 9a, referred to FSV index, Instead, it is largely extended for YMV index (Fig. 9b).

Summarizing, this study assesses the promising use of Fiber-Reinforced Composites (FFRCs) in specific outdoor applications where they can act as semi-structural elements. However, a potential issue of permanent stiffness loss due to alternate hydrothermal aging needs careful attention. This highlights the importance of further research into improving FFRC durability under fluctuating humidity and dryness conditions. Thus, the study emphasizes the need for more comprehensive knowledge on FFRCs durability to guarantee their long-term performance and reliability in real-world settings.

3.3. Performance recovery modelling

With the purpose to assess the performances degradation and recovery of the composite during humid/dry cycles, an analytical model able to explain the recovery process of the investigated composites was proposed, considering how their alternate aging influences this behavior. This model aims to identify the key characteristics of the recovery phenomenon for all the materials studied.

When composites are exposed to humidity, their mechanical properties can significantly change due to processes like plasticization and weakening of the fiber-matrix bond. Besides, the performance degradation can be related to weight changes in composites resulting from water absorption and desorption occurring during humid/dry cycles [49,50]. To validate this statement, the relationships between flexural strength and modulus and weight change values during humid and dry phases of each cycle were reported in Fig. 10 (a) and (b) respectively.

Regardless of the aging cycle number, a quite linear trend with both flexural strength and elastic modulus values reduced proportionally with the weight gain was identified. This means that materials with larger weight gains experienced larger reductions in their mechanical strength and stiffness.

The release of water during the drying phase is linked to a gradual process of releasing absorbed water molecules. As a result, the main reason for the performance recovery of composites dried after being exposed to the humid environment can be likely related to the removal of water vapor from the material's core by desorption. In this concern, a pseudo-second-order model could be applied to predict their evolution during time [51,52], allowing to define a performance recovery model based on this approach [53]. In particular:

$$\frac{dX_t}{dt} = K_2(X_e - X_t)^2 \tag{3}$$

Where X_t is the performance recovery (expressed in MPa or GPa for strength and modulus respectively) at a specific time t. If we integrate Equation (3) considering the starting condition that the concentration of X (denoted by X_t) is 0 at time 0 (t = 0), and the ending condition that Xt reaches a specific value (X_t) at a specific time (t = t), we can transform the resulting expression for pseudo-second-order kinetics into a linear form.

$$\frac{t}{X_t} = \frac{1}{K_2 X_e^2} + \frac{t}{X_e} \tag{4}$$

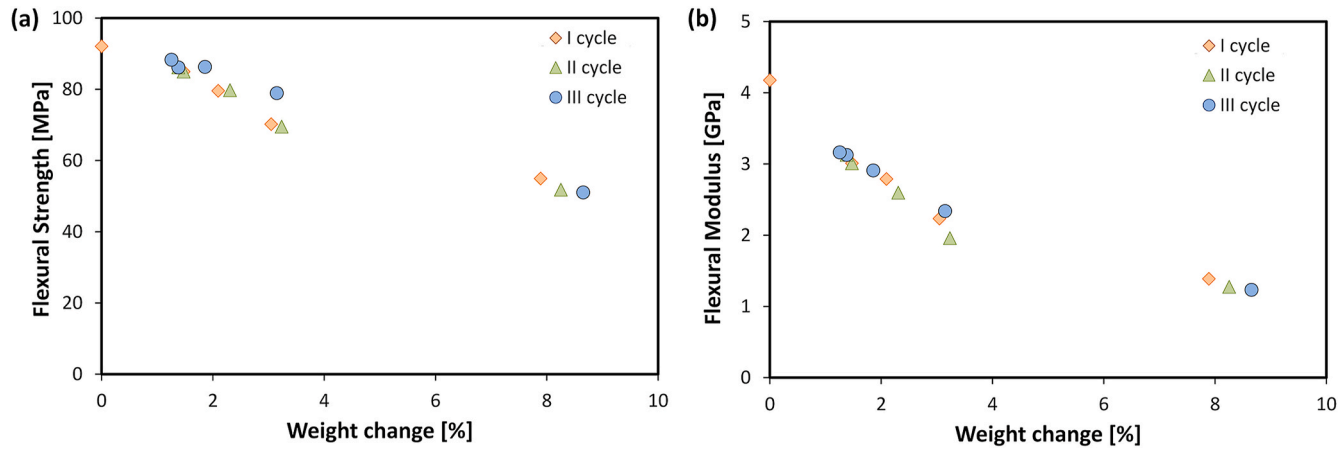

Fig. 10. (a) Flexural strength and (b) modulus versus weight change.

the second-order rate constant K_2 ($MPa^{-1}\cdot h^{-1}$) and the maximum equilibrium performance recovery (X_e) can be determined from the slope and intercept of a linear plot of t/X_t versus time. Additionally, the initial performance recovery rate $h_{0,2}$ (MPa h^{-1}) and the half performance recovery time h can be calculated using the following equations:

$$h_{o,2} = K_2 X_e^2 \tag{5}$$

$$t_{1/2} = \frac{1}{K_2 \cdot X_e} \tag{6}$$

Based on this analysis, a relationship between performance recovery and drying time can be assessed by examining the fitting parameters presented in Table 3.

The composite samples exposed to aging cycles show inconsistent data, making it difficult to identify a clear trend across the three batches. Possibly, this is likely due to limited aging cycles that don't sufficiently distinguish between performance changes among the batches. However, some insights are available:

Maximum recovery: After the third aging cycle, the maximum equilibrium performance recovery (X_e) is notably higher than after the first cycle for both flexural strength and modulus. This suggests that highly aged samples recover better when transitioning from humid to dry phases compared to low aging cycle samples.

Recovery rate: Samples exposed to three aging cycles show a significantly faster initial performance recovery rate ($h_{0,2}$ parameter) in flexural strength compared to those exposed to a single cycle.

Exposing materials to repeated cycles of humid/dry cycles for extended periods impacts how they release water by desorption and, consequently, how well they recover their lost mechanical performance. This effect is more pronounced in materials that suffered aging and developed preferential pathways for water diffusion, as previously discussed.

These pathways allow water to move through the material more easily and quickly during the drying phase, leading to a faster and more complete recovery of mechanical performance. This applies to both the speed of recovery and the extent of performance regained after a long drying period.

However, this consideration, valid for flexural strength parameter, is less relevant for the flexural modulus parameter. This is because cracks, debonding and delamination caused by the humid phases can permanently damage the material, hindering its ability to recover its original performance [25]. Furthermore, the presence of these defects, such as delamination, debonding voids, or micro-cracks, in natural fiber composites significantly delays performance recovery during subsequent drying phases [21]. This, in turns, leads to a significantly lower $h_{0,2}$ value compared to the flexural modulus parameter.

Based on the achieved experimental data and the theoretical model we propose a simplified method to predict the mechanical behavior of the composite material when exposed to alternating humid and dry conditions (humid/dry cycle). This method considers that we observe a decline in the mechanical performance during the humid phase, followed by a partial recovery during the dry phase. Indicating as P_0 the initial value of a specific flexural property (e.g., strength or modulus) of composite before any exposure to humid/dry cycles; we can estimate the mechanical performance (P_t) of the composite at any given time (t) after the start of the humid/dry cycle, $P_t = P_{(th+td)}$, as:

$$P_{(th+td)} = P_0 \frac{\alpha_h(t_h)}{\alpha_d(t_d)} \tag{7}$$

This simplified formula was define considering that the effectiveness of a material exposed to a harsh environment, like salt-fog, can degrade over time. This degradation is represented by the decay factor, $\alpha_h(t_h)$, which is related to the material's exposure duration, t_h. Conversely, the material can recover some of its effectiveness when placed in a dry environment. This recovery is captured by the recovery factor, $\alpha_d(t_d)$, which is related to the drying time, t_d. It's important to note that both decay and recovery factors are always less than 1. The decay factor and recovery factor are defined by the following expression, respectively:

$$\alpha_h(t_h) = \frac{P_h@t_h}{P_0} \tag{8}$$

$$\alpha_d(t_d) = \frac{P_h}{P_h@t_h + X_d@t_d} \tag{9}$$

Where $P_h@t_h$ is the mechanical performance (i.e., strength or modulus) at t_h exposition time related to the humid phase and it was calculated by considering the linear relationship between mechanical performance and water uptake [54], by using the following equation:

$$P_h@t_h = \left(1 - \frac{P_0 - P_{h\infty}}{P_0}\frac{WC_{t_h}}{WC_\infty}\right)P_0 \tag{10}$$

Table 3
Pseudo-second order fitting parameters.

			I Cycle	II Cycle	III Cycle
Flexural Strength	X_e	MPa	32.294	36.809	38.219
	K_2	$MPa^{-1}\cdot h^{-1}$	0.0005	0.0005	0.0013
	$h_{0,2}$	MPa/h	0.527	0.613	1.971
	$t_{1/2}$	h	0.928	0.931	0.992
Flexural Modulus	X_e	MPa	1.746	2.043	2.115
	K_2	$MPa^{-1}\cdot h^{-1}$	0.0103	0.0041	0.0108
	$h_{0,2}$	MPa/h	0.031	0.018	0.045
	$t_{1/2}$	h	0.936	0.783	0.958

$P_{h\infty}$ is the reduced performance at maximum exposition time (10 days of humid exposition). WC_{t_h} and WC_∞ are the weight change values observed at t_h and at maximum exposition, respectively. Instead, $X_d@t_d$, is the mechanical performance (i.e., strength or modulus) at t_d exposition time in the dry environment and can be determined based on eq. (4). Fig. 11 evaluates the effectiveness of the proposed mathematical model by comparing and the fitting results and the experimental data. The data are referred to the three-point bending strength and stiffness (i.e., modulus) values shown by flax fiber reinforced composite during the dry phases of each cycle (i.e., I, II and III).

The provided graphs suggest that the simplified forecasting model accurately predicts both flexural strength and modulus of the composite throughout the entire drying period, regardless of the duration of the humid phase. The model closely matches the experimental data at short and long drying times. However, a small discrepancy emerges at intermediate times (around 120 h), where deviations of about 8 % and 15 % in flexural strength and modulus trends, respectively, are observed. This drying time coincides with a "knee" in the recovery trend, indicating a transition from kinetically fast to diffusion-limited recovery mechanisms. Nevertheless, the good fit is further confirmed by the low root mean squared error (RMSE) [55]. The RMSE between the predicted and experimental values indicated a high degree of fit, supported by an average R-squared value (R^2 or the coefficient of determination) of at least 0.85, demonstrating the pseudo-second order model's accuracy regardless the applied aging cycle.

4. Conclusion

This study examines the impact of multiple humid-dry aging cycles on the mechanical stability and physical properties of flax fiber reinforced composites (FFRCs) with the main aim of assessing their durability in simulated outdoor conditions, also promoting sustainable composites for semi-structural applications. To this scope, FFRCs were aged for 12 weeks by exposing them to three repeated humid (salt-fog)/dry cycles.

It was found that the investigated composites show weight gain during the humid phase of each repeated cycle, followed by weight loss upon each drying phase. More in detail, the maximum water uptake values improve at the end of each humid phase as well as the residual

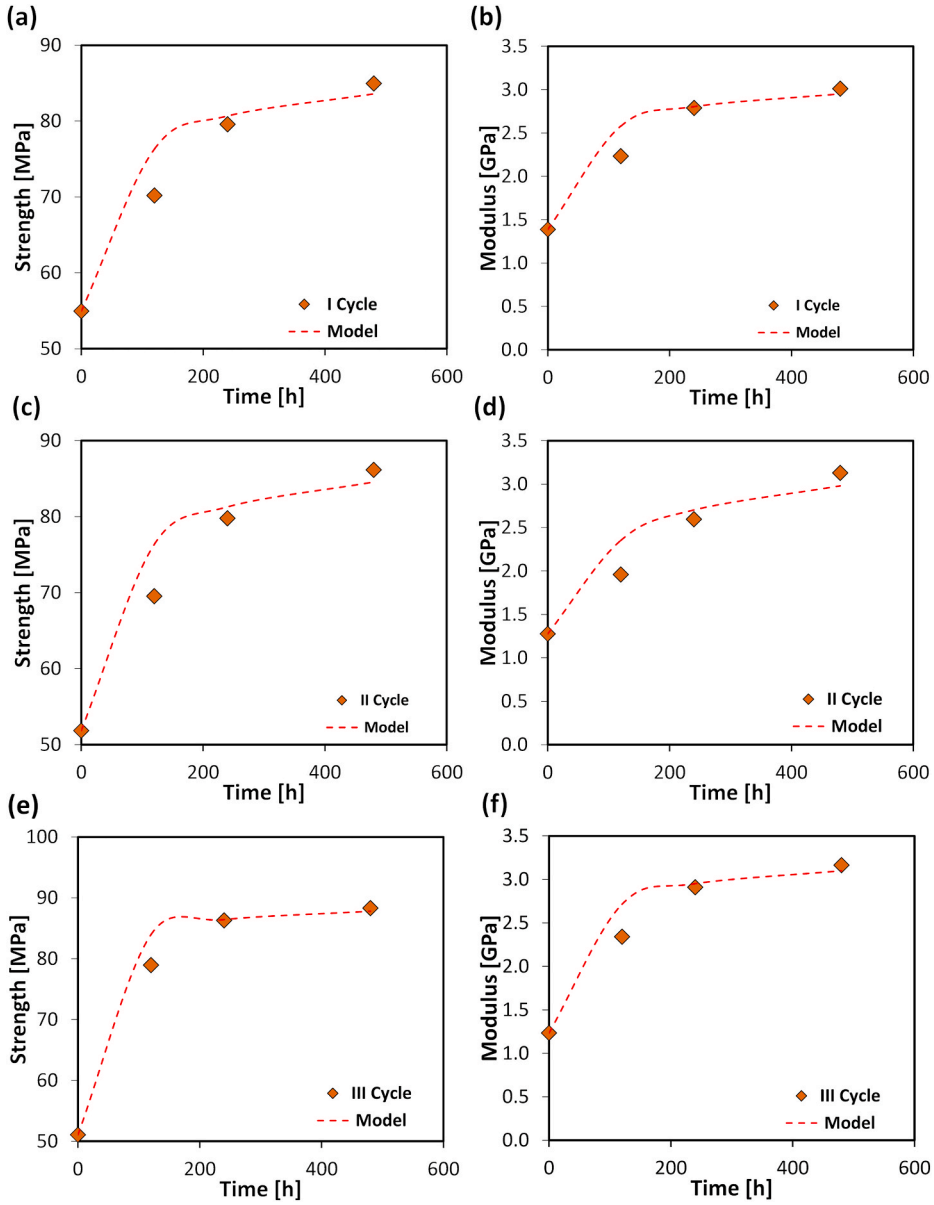

Fig. 11. Experimental data and model fitting results referred to (a, c, e) flexural strength and (b, d, f) modulus during dry phases of each aging cycle.

weight values reduce at the end of each dry phase, with increasing the number of cycles. Therefore, a greater gap between maximum and minimum weight uptake values was evidenced as a function of the aging cycle' number, mainly due to the degradation phenomena that occurred during the salt-fog exposition, which become more relevant as the number of applied cycles increases.

From the mechanical point of view, FFRCs weaken when exposed to the salt-fog environment, but they were also able to recover their mechanical stability during the next dry phases of each cycle, regaining 20–30 % of strength after few days. This means that the strength reduction is almost full reversible. However, the flexural modulus of composites exposed to three aging cycles (i.e., at the end of the aging campaign) remained −24 % lower than that of unaged ones.

Furthermore, an analytical simplified model was proposed to assess the performance degradation and recovery shown by FFRCs exposed to multiple humid/dry cycles. It allowed us to understand with promising effectiveness how non-constant aging conditions can affect the recovery process and identifying key characteristics of this phenomenon in the studied materials.

Overall, this paper addresses the potential of FFRCs for specific semi-structural outdoor applications. However, concerns arise regarding permanent stiffness loss caused by accelerated aging, requiring careful consideration. This stresses the need to further developing their aging resistance when exposed to alternate humid/dry environmental conditions. The achieved findings underline the relevance of advancing and improving the current knowledge on FFRCs durability to ensure their long-term effectiveness and reliability in real-world scenarios.

CRediT authorship contribution statement

V. Fiore: Writing – review & editing, Resources, Data curation. **L. Calabrese:** Writing – review & editing, Methodology, Data curation, Conceptualization. **C. Sanfilippo:** Writing – original draft, Investigation, Data curation. **E. Proverbio:** Supervision, Project administration, Funding acquisition. **A. Valenza:** Supervision, Project administration, Funding acquisition.

Declaration of competing interest

The authors declare that they have no known competing financial interests or personal relationships that could have appeared to influence the work reported in this paper.

Data availability

Data will be made available on request.

Acknowledgements

This work was developed in the framework of the project "SI-MARE – Soluzioni Innovative per Mezzi navali ad Alto Risparmio Energetico" (P. O. FESR Sicilia 2014/2020, grant number 08ME7219090182).

References

[1] S. Sinha, G.L. Devnani, Natural fiber composites, in: Processing, Characterization, Applications, and Advancements, CRC Press, Boca Raton, 2022, https://doi.org/10.1201/9781003201724.
[2] N. Nurhania, S. Syarifuddin, B. Armynah, D. Tahir, Fiber-reinforced polymer composite: higher performance with renewable and eco-friendly plant-based fibers, Polym. Renew. Resour. 14 (2023) 215–233, https://doi.org/10.1177/20412479231173113.
[3] A. Samal, S. Kumar, P.K.S. Mural, M. Bhargava, S.N. Das, J.K. Katiyar, A critical review of different properties of natural fibre-reinforced composites, Proc. Inst. Mech. Eng. Part E J Process Mech Eng (2023) 09544089231202915, https://doi.org/10.1177/09544089231202915.
[4] M. Demir, R. Ekici, Investigation of low-velocity impact behaviors of polymer composites reinforced with different natural fiber fabrics, Polym. Compos. 45 (2024) 4928–4946, https://doi.org/10.1002/pc.28099.
[5] M. Karahan, F. Ozkan, K. Yildirim, N. Karahan, Investigation of the properties of natural fibre woven fabrics as a reinforcement materials for green composites, Fibres Text. East. Eur. 24 (2016) 98–104, https://doi.org/10.5604/12303666.1201138.
[6] H.A. Aisyah, M.T. Paridah, S.M. Sapuan, R.A. Ilyas, A. Khalina, N.M. Nurazzi, et al., A comprehensive review on advanced sustainable woven natural fibre polymer composites, Polymers 13 (2021) 1–45, https://doi.org/10.3390/polym13030471.
[7] H. Abdollahiparsa, A. Shahmirzaloo, P. Teuffel, R. Blok, A review of recent developments in structural applications of natural fiber-Reinforced composites (NFRCs), Compos. Adv. Mater. 32 (2023) 26349833221147540, https://doi.org/10.1177/26349833221147540.
[8] M.F.E. Silva, B.R. Silva, A.N. Marques, S. Mattedi, R.F. Carvalho, Effect of hydrothermal aging on damping properties in sisal mat-reinforced polyester composites, Polymers 16 (2024), https://doi.org/10.3390/polym16020166.
[9] A. Le Duigou, T. Fruleux, R. Matsuzaki, G. Chabaud, M. Ueda, M. Castro, 4D printing of continuous flax-fibre based shape-changing hygromorph biocomposites: towards sustainable metamaterials, Mater. Des. 211 (2021), https://doi.org/10.1016/j.matdes.2021.110158.
[10] A. Le Duigou, V. Keryvin, J. Beaugrand, M. Pernes, F. Scarpa, M. Castro, Humidity responsive actuation of bioinspired hygromorph biocomposites (HBC) for adaptive structures, Composites Part A Appl Sci Manuf 116 (2019), https://doi.org/10.1016/j.compositesa.2018.10.018.
[11] Q. Wang, T. Chen, X. Wang, Y. Zheng, J. Zheng, G. Song, et al., Recent progress on moisture absorption aging of plant fiber reinforced polymer composites, Polymers 15 (2023), https://doi.org/10.3390/polym15204121.
[12] T.H. Mokhothu, M.J. John, Review on hygroscopic aging of cellulose fibres and their biocomposites, Carbohydr. Polym. 131 (2015) 337–354, https://doi.org/10.1016/j.carbpol.2015.06.027.
[13] M.H. Ameer, K. Shaker, M. Ashraf, M. Karahan, Y. Nawab, S. Ahmad, et al., Interdependence of moisture, mechanical properties, and hydrophobic treatment of jute fibre-reinforced composite materials, J. Text. Inst. 108 (2017) 1768–1776, https://doi.org/10.1080/00405000.2017.1285201.
[14] H.J. Kim, D.W. Seo, Effect of water absorption fatigue on mechanical properties of sisal textile-reinforced composites, Int. J. Fatig. 28 (2006) 1307–1314, https://doi.org/10.1016/j.ijfatigue.2006.02.018.
[15] B. Zuccarello, C. Militello, F. Bongiorno, Environmental aging effects on high-performance biocomposites reinforced by sisal fibers, Polym. Degrad. Stabil. 211 (2023), https://doi.org/10.1016/j.polymdegradstab.2023.110319.
[16] T. Cadu, L. Van Schoors, O. Sicot, S. Moscardelli, L. Divet, S. Fontaine, Cyclic hygrothermal ageing of flax fibers' bundles and unidirectional flax/epoxy composite. Are bio-based reinforced composites so sensitive? Ind. Crops Prod. 141 (2019) 111730 https://doi.org/10.1016/j.indcrop.2019.111730.
[17] L. Van Schoors, T. Cadu, S. Moscardelli, L. Divet, S. Fontaine, O. Sicot, Why cyclic hygrothermal ageing modifies the transverse mechanical properties of a unidirectional epoxy-flax fibres composite? Ind. Crops Prod. 164 (2021) 113341 https://doi.org/10.1016/j.indcrop.2021.113341.
[18] K. Mak, A. Fam, The effect of wet-dry cycles on tensile properties of unidirectional flax fiber reinforced polymers, Composites, Part B 183 (2020) 107645, https://doi.org/10.1016/j.compositesb.2019.107645.
[19] R. Barbière, F. Touchard, L. Chocinski-Arnault, D. Mellier, Influence of moisture and drying on fatigue damage mechanisms in a woven hemp/epoxy composite: acoustic emission and micro-CT analysis, Int. J. Fatig. 136 (2020) 105593, https://doi.org/10.1016/j.ijfatigue.2020.105593.
[20] L. Calabrese, V. Fiore, E. Piperopoulos, D. Badagliacco, D. Palamara, A. Valenza, et al., In situ monitoring of moisture uptake of flax fiber reinforced composites under humid/dry conditions, J. Appl. Polym. Sci. 139 (2022) 51969, https://doi.org/10.1002/app.51969.
[21] V. Fiore, L. Calabrese, R. Miranda, D. Badagliacco, C. Sanfilippo, D. Palamara, et al., On the response of flax fiber reinforced composites under salt-fog/dry conditions: reversible and irreversible performances degradation, Composites, Part B 230 (2022) 109535, https://doi.org/10.1016/j.compositesb.2021.109535.
[22] L. Calabrese, D. Badagliacco, C. Sanfilippo, V. Fiore, Flax-glass fiber reinforced hybrid composites exposed to a salt-fog/dry cycle: a simplified approach to predict their performance recovery, Polymers 15 (2023), https://doi.org/10.3390/polym15112542.
[23] V. Fiore, L. Calabrese, R. Miranda, D. Badagliacco, C. Sanfilippo, D. Palamara, et al., Assessment of performance degradation of hybrid flax-glass fiber reinforced epoxy composites during a salt spray fog/dry aging cycle, Composites, Part B 238 (2022), https://doi.org/10.1016/j.compositesb.2022.109897.
[24] L. Calabrese, V. Fiore, A. Valenza, E. Proverbio, A topological weakening and softening map as simplified tool to assess the performances recovery of hybridized natural fiber reinforced composites subjected to alternate salt-fog/dry cycle, Polym. Test. 127 (2023) 108186, https://doi.org/10.1016/j.polymertesting.2023.108186.
[25] V. Fiore, L. Calabrese, R. Miranda, D. Badagliacco, C. Sanfilippo, D. Palamara, et al., An experimental investigation on performances recovery of glass fiber reinforced composites exposed to a salt-fog/dry cycle, Composites, Part B 257 (2023) 110693, https://doi.org/10.1016/j.compositesb.2023.110693.
[26] L. Calabrese, V. Fiore, R. Miranda, D. Badagliacco, C. Sanfilippo, D. Palamara, et al., Performances recovery of flax fiber reinforced composites after salt-fog aging test, J Compos Sci 6 (2022) 1–12, https://doi.org/10.3390/jcs6090264.
[27] M. Karahan, N. Karahan, Influence of weaving structure and hybridization on the tensile properties of woven carbon-epoxy composites, J. Reinforc. Plast. Compos. 33 (2014) 212–222, https://doi.org/10.1177/0731684413504019.

[28] J. Zhou, J.P. Lucas, Hygrothermal effects of epoxy resin. Part I: the nature of water in epoxy, Polymer 40 (1999) 5505–5512, https://doi.org/10.1016/S0032-3861(98)00790-3.
[29] S.K. Karad, D. Attwood, F.R. Jones, Moisture absorption by cyanate ester modified epoxy resin matrices. Part V: effect of resin structure, Composites Part A Appl Sci Manuf 36 (2005) 764–771, https://doi.org/10.1016/j.compositesa.2004.10.022.
[30] A. Moudood, A. Rahman, A. Öchsner, M. Islam, G. Francucci, Flax fiber and its composites: an overview of water and moisture absorption impact on their performance, J. Reinforc. Plast. Compos. 38 (2019) 323–339, https://doi.org/10.1177/0731684418818893.
[31] M. Assarar, D. Scida, A. El Mahi, C. Poilâne, R. Ayad, Influence of water ageing on mechanical properties and damage events of two reinforced composite materials: flax-fibres and glass-fibres, Mater. Des. 32 (2011) 788–795, https://doi.org/10.1016/j.matdes.2010.07.024.
[32] A. Moudood, A. Rahman, H.M. Khanlou, W. Hall, A. Öchsner, G. Francucci, Environmental effects on the durability and the mechanical performance of flax fiber/bio-epoxy composites, Composites, Part B 171 (2019) 284–293, https://doi.org/10.1016/j.compositesb.2019.05.032.
[33] H.N. Dhakal, Z.Y. Zhang, M.O.W. Richardson, Effect of water absorption on the mechanical properties of hemp fibre reinforced unsaturated polyester composites, Compos. Sci. Technol. 67 (2007) 1674–1683, https://doi.org/10.1016/j.compscitech.2006.06.019.
[34] A. Stamboulis, C.A. Baillie, T. Peijs, Effects of environmental conditions on mechanical and physical properties of flax fibers, Composites Part A Appl Sci Manuf 32 (2001) 1105–1115, https://doi.org/10.1016/S1359-835X(01)00032-X.
[35] J. Mercier, A. Bunsell, P. Castaing, J. Renard, Characterisation and modelling of aging of composites, Composites Part A Appl Sci Manuf 39 (2008) 428–438, https://doi.org/10.1016/j.compositesa.2007.08.015.
[36] R.H. Newman, Auto-accelerative water damage in an epoxy composite reinforced with plain-weave flax fabric, Composites Part A Appl Sci Manuf 40 (2009) 1615–1620, https://doi.org/10.1016/j.compositesa.2009.07.010.
[37] L. Calabrese, V. Fiore, P.G. Bruzzaniti, T. Scalici, A. Valenza, An aging evaluation of the bearing performances of glass fiber composite laminate in salt spray fog environment, Fibers 7 (2019), https://doi.org/10.3390/fib7110096.
[38] C.J. Tsenoglou, S. Pavlidou, C.D. Papaspyrides, Evaluation of interfacial relaxation due to water absorption in fiber–polymer composites, Compos. Sci. Technol. 66 (2006) 2855–2864, https://doi.org/10.1016/j.compscitech.2006.02.022.
[39] T. Haghighatnia, A. Abbasian, J. Morshedian, Hemp fiber reinforced thermoplastic polyurethane composite: an investigation in mechanical properties, Ind. Crops Prod. 108 (2017) 853–863, https://doi.org/10.1016/j.indcrop.2017.07.020.
[40] L. Calabrese, V. Fiore, T. Scalici, A. Valenza, Experimental assessment of the improved properties during aging of flax/glass hybrid composite laminates for marine applications, J. Appl. Polym. Sci. 136 (2019) 47203, https://doi.org/10.1002/app.47203.
[41] L. Yan, Effect of alkali treatment on vibration characteristics and mechanical properties of natural fabric reinforced composites, J. Reinforc. Plast. Compos. 31 (2012) 887–896, https://doi.org/10.1177/0731684412449399.
[42] M. Habibi, G. Lebrun, L. Laperrière, Experimental characterization of short flax fiber mat composites: tensile and flexural properties and damage analysis using acoustic emission, J. Mater. Sci. 52 (2017) 6567–6580, https://doi.org/10.1007/s10853-017-0892-1.
[43] V. Fiore, L. Calabrese, T. Scalici, A. Valenza, Evolution of the bearing failure map of pinned flax composite laminates aged in marine environment, Composites, Part B 187 (2020) 107864, https://doi.org/10.1016/j.compositesb.2020.107864.
[44] D. Ray, J. Rout, Thermoset biocomposites, in: Nat. Fibers, Biopolym. Biocomposites, CRC Press, 2005, pp. 291–345, https://doi.org/10.1201/9780203508206.ch9.
[45] T. Alomayri, H. Assaedi, F.U.A. Shaikh, I.M. Low, Effect of water absorption on the mechanical properties of cotton fabric-reinforced geopolymer composites, J Asian Ceram Soc 2 (2014) 223–230, https://doi.org/10.1016/j.jascer.2014.05.005.
[46] Z.N. Azwa, B.F. Yousif, A.C. Manalo, W. Karunasena, A review on the degradability of polymeric composites based on natural fibres, Mater. Des. 47 (2013) 424–442, https://doi.org/10.1016/j.matdes.2012.11.025.
[47] C. Maggana, P. Pissis, Water sorption and diffusion studies in an epoxy resin system, J. Polym. Sci., Part B: Polym. Phys. 37 (1999) 1165–1182, https://doi.org/10.1002/(SICI)1099-0488(19990601)37:11<1165::AID-POLB11>3.0.CO;2-E.
[48] A. Chilali, W. Zouari, M. Assarar, H. Kebir, R. Ayad, Effect of water ageing on the load-unload cyclic behaviour of flax fibre-reinforced thermoplastic and thermosetting composites, Compos. Struct. 183 (2018) 309–319, https://doi.org/10.1016/J.COMPSTRUCT.2017.03.077.
[49] I.B.C.M. Rocha, F.P. van der Meer, S. Raijmaekers, F. Lahuerta, R.P.L. Nijssen, L. J. Sluys, Numerical/experimental study of the monotonic and cyclic viscoelastic/viscoplastic/fracture behavior of an epoxy resin, Int. J. Solid Struct. 168 (2019) 153–165, https://doi.org/10.1016/j.ijsolstr.2019.03.018.
[50] F. Naya, C. González, C.S. Lopes, S. Van der Veen, F. Pons, Computational micromechanics of the transverse and shear behavior of unidirectional fiber reinforced polymers including environmental effects, Composites Part A Appl Sci Manuf 92 (2017) 146–157, https://doi.org/10.1016/j.compositesa.2016.06.018.
[51] W.K. Mekhamer, Energy storage through adsorption and desorption of water vapour in raw Saudi bentonite, Arab. J. Chem. 9 (2016) S264–S268, https://doi.org/10.1016/j.arabjc.2011.03.021.
[52] Q. Zeng, D. Zhang, K. Li, Kinetics and equilibrium isotherms of water vapor adsorption/desorption in cement-based porous materials, Transport Porous Media 109 (2015) 469–493, https://doi.org/10.1007/s11242-015-0531-8.
[53] Y.-S. Ho, Review of second-order models for adsorption systems, J. Hazard Mater. 136 (2006) 681–689, https://doi.org/10.1016/j.jhazmat.2005.12.043.
[54] I.B.C.M. Rocha, F.P. van der Meer, S. Raijmaekers, F. Lahuerta, R.P.L. Nijssen, L. P. Mikkelsen, et al., A combined experimental/numerical investigation on hygrothermal aging of fiber-reinforced composites, Eur. J. Mech. Solid. 73 (2019) 407–419, https://doi.org/10.1016/j.euromechsol.2018.10.003.
[55] A.K. Vanhari, E. Fagan, J. Goggins, A novel estimation method for fitting fatigue data in the composite wearout model, Compos. Struct. 287 (2022) 115384, https://doi.org/10.1016/j.compstruct.2022.115384.